2024 IEEE 63rd Conference on Decision and Control (CDC)
December 16-19, 2024. MiCo, Milan, Italy

Stable Dynamic Residual-Neural-Network-Based Estimator for Unknown Nonlinearities and Disturbances

Pan Yu, Qiang Wu

Abstract— **Using only the system output, a stable dynamic residual-neural-network-based (DRNN-based) estimator with excellent learning ability is devised to deal with unknown nonlinearities and disturbances of control systems. First, the unknown nonlinearities and disturbances are treated as a lumped disturbance, and an auxiliary variable is introduced to indicate the adverse impact on the system output. Then, to suppress this impact, a stable DRNN is organically integrated into a conventional equivalent-input-disturbance (EID) estimator to enhance the learning or estimation ability for the lumped disturbance. As for interpretability, the feed-forward neural network (NN) term can be viewed as a dynamic learning compensator, which is optimized by the backpropagation algorithm, and the residual term can be viewed as a performance-oriented adaptive learning gain. The stability of the DRNN-based estimator is guaranteed. Finally, comparisons with a conventional EID-based method show the developed learning method has an incomparable dynamic performance in a case study of a single-joint robot.**

I. Introduction

Unknown nonlinearities and disturbances widely exist in practical systems [1]. Developing effective strategies is crucial to improving system performance in applications like robotics, aerospace, and smart grids.

Despite the differences between nonlinearities and disturbances, treating nonlinearities as disturbances allows the transformation of the challenge of nonlinear control into the problem of disturbance rejection. Accordingly, numerous methods designed for disturbance rejection are applicable to tackle both nonlinearities such as classic control methods (e.g. H_∞ control [2] and sliding-mode control [3]) and active disturbance-rejection (ADR) methods based on disturbance estimation and compensation (e.g. the disturbance observer (DOB) [4], the extended-state observer (ESO) [5], and the equivalent-input-disturbance (EID) approach [6]).

The DOB in the frequency domain employs an inverse of a plant together with a filter to estimate disturbances of linear systems [7]. It is not easy to formulate the filter due to the multiple constraints of causality, stability, and control performance. A nonlinear disturbance observer (NDOB) was presented to compensate for disturbances in a nonlinear system [8]. It required system states and disturbance information. Viewing nonlinearities and disturbances as an extended state of a control system, the ESO estimates the lumped disturbance together with the system states [9]. However, the ESO requires the match condition for disturbances. This may narrow the range of its applications.

Using the EID concept, the EID estimator effectively implements disturbance-rejection control through the reconstruction of an artificial disturbance, known as an EID, which is defined on the control input channel and has the same effect as real lumped disturbances on the system output [10]. The EID approach is effective for both matched and mismatched nonlinearities and disturbances. It has been widely used [11], [12].

In recent years, owing to the powerful learning and adaptive ability, neural networks (NNs) have been widely used in several fields. For instance, metaheuristic algorithms were incorporated into recurrent NNs to solve prediction and optimization problems of kinematic control of redundant mobile manipulators [13], [14]. However, these results are mostly limited to open-loop applications. Integrating NN algorithms into the closed-loop system remains a challenge for improving the control and learning performance of dynamic systems.

In this paper, a dynamic residual neural network (DRNN) is organically integrated into the analysis and synthesis of an EID-based control system with unknown nonlinearities and disturbances. To be specific, a stable DRNN-based estimator is developed, which capitalizes on the learning capabilities of NNs and has remarkable control performance compared with classic control theory methods. Moreover, the uniformly ultimately bounded stability is guaranteed for the closed-loop learning control system. The main novelties of this paper are listed as follows.

- In order to evaluate the learning or estimation effect for unknown nonlinearities and disturbances, an auxiliary indicator is first introduced.
- A performance-oriented adaptive learning law with stability guarantee is devised for the residual term of the DRNN.
- The feed-forward neural network (NN) component serves as a learning compensator, improving dynamic estimation performance through backpropagation optimization.

In this paper, $\mathbb{R}^{m\times n}$ denotes the set of real matrices with m rows and n columns; $P = P^T > 0$ means P is a positive-definite symmetric matrix; $\mathrm{trace}(A)$, $\lambda_{\max}(A)$ and $\lambda_{\min}(A)$ denote the sum of diagonal elements, the maximum and minimum eigenvalue of the matrix A, respectively; $|a|$ denotes the absolute value of a scalar a; and $\|x\|$ denotes the norm of a vector or matrix x.

This work was supported in part by the National Natural Science Foundation of China under Grant 62003010 and in part by the R&D Program of Beijing Municipal Education Commission under Grant KM202410005036. (Corresponding author: Pan Yu.)

P. Yu and Qiang Wu are with the School of Information Science and Technology, the Beijing Institute of Artificial Intelligence, Beijing University of Technology, Beijing 100124, China (Email: panyu@bjut.edu.cn, wuqiang@emails.bjut.edu.cn).

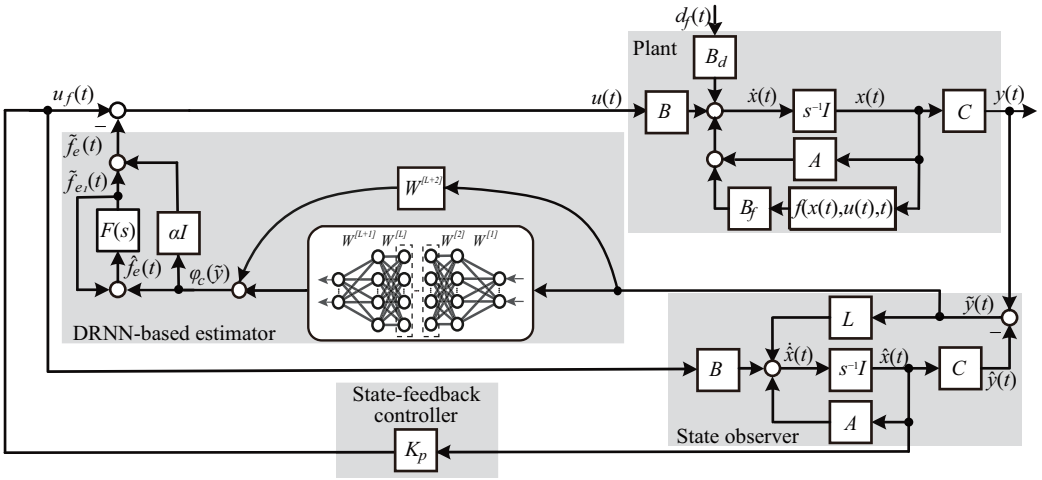

Fig. 1. Configuration of DRNN-based control system

II. System Configuration

The configuration of the developed control system is shown in Fig. 1. It mainly has four parts: a plant, a state observer, a DRNN-based estimator, and a state-feedback controller.

Consider the following system

$$\begin{cases} \dot{x}(t) = Ax(t) + Bu(t) + B_f f(x(t),u(t),t) + B_d d_f(t) \\ y(t) = Cx(t) \end{cases} \tag{1}$$

where $x(t) \in \mathbb{R}^n$ is the system state; $u(t), y(t) \in \mathbb{R}$ are the control input, system output, respectively; $f(x(t),u(t),t) \in \mathbb{R}^{n_f}$ is a function including nonlinearities and internal uncertainties of the system; $d_f(t)$ is an exogenous disturbance; and A, B, B_f, B_d, and C are real constant matrices with compatible dimensions.

Assumption 1: (A,B) is controllable and (A,C) is observable.

Assumption 2: (A,B,C) has no zeros on the closed left half of the complex plane.

Assumption 3: For any $x(t)$, $z(t) \in \mathbb{R}^n$, the nonlinear function $f(x(t),u(t),t)$ satisfies $f(0,0,t) = 0$ and

$$\|f(x(t),u(t),t) - f(z(t),u(t),t)\| \le R\|(x(t) - z(t))\| \tag{2}$$

where R is a positive number.

Assumption 4: The $d_f(t)$ satisfies

$$|d_f(t)| \le d_m, \quad t \ge 0 \tag{3}$$

where d_m is an unknown but bounded positive number.

A full-order state observer is constructed to approximate the states of the plant (1) by

$$\begin{cases} \dot{\hat{x}}(t) = A\hat{x}(t) + Bu_f(t) + L(y(t) - \hat{y}(t)) \\ \hat{y}(t) = C\hat{x}(t) \end{cases} \tag{4}$$

where $\hat{x}(t)$, $u_f(t)$, and $\hat{y}(t)$ denote the state, input, and output of the observer, respectively; and L represents the observer gain that needs to be determined.

The feedback control law $u_f(t)$ is expressed as

$$u_f(t) = K_p\hat{x}(t). \tag{5}$$

Denote $\tilde{f}_e(t)$ as the EID estimate of the DRNN-based estimator. The details about the DRNN-based estimator are given in the next section. Integrating the EID estimate $\tilde{f}_e(t)$ into the feedback control law $u_f(t)$ yields

$$u(t) = u_f(t) - \tilde{f}_e(t). \tag{6}$$

III. Auxiliary Impact Indicator of Lumped Disturbance

Due to the unknown of the nonlinearities and disturbances, it is difficult to uncover their impact on the control system directly. It is well known that an observer can be viewed as a copy version of a control system where there are no nonlinearities and disturbances.

By substituting (5) into (4), the dynamics of the observer can be rewritten as

$$\dot{\hat{x}}(t) = A_K\hat{x}(t) + L\tilde{y}(t) \tag{7}$$

where

$$\tilde{y}(t) = y(t) - \hat{y}(t) \tag{8}$$

and

$$A_K = A + BK_p. \tag{9}$$

Further, according to (8), we have

$$y(t) = C\hat{x}(t) + \tilde{y}(t). \tag{10}$$

Therefore, by the auxiliary variable $\tilde{y}$, the impact of the nonlinearities and disturbances on the system output can be seen from the observer dynamics (7) together with its system output equation (10). Further, when $\tilde{y}$ is zero, the impact of the nonlinearities and disturbances vanishes.

As a result, the deviation of $\tilde{y}$ from the origin indicates the impact of the unknown nonlinearities and disturbances on the system output in a way.

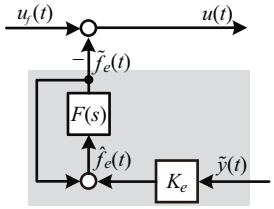

Fig. 2. Conventional EID estimator.

IV. DRNN-BASED ESTIMATOR

A conventional EID estimator is recalled in this section and then the developed DRNN-based estimator is introduced.

A. Conventional EID Estimator

Based on the EID concept, the control idea of EID estimators is to reconstitute an EID estimate and feed it back to the control input channel. Different from the GESO, the EID estimator does not require the coordination gain and is regardless of both matched and mismatched disturbances, since the estimate is acted on the control input channel.

The conventional EID estimator is shown in Fig. 2, where the filter is used to select the angular frequency for estimation and K_e is a control gain [15].

B. Novel DRNN-based Estimator

To incorporate the strong learning ability of NN into EID estimators, a DRNN-based estimator is constructed as shown in Fig. 1, which consists of a feed-forward NN and a residual term. Moreover, a parameter α is introduced to enhance the stability.

The output of the DRNN is

$$\varphi_c(\tilde{y}) = W^{[2]}h(W^{[1]}\tilde{y}) + W^{[3]}\tilde{y} \tag{11}$$

where $W^{[1]}, W^{[2]}$ are the weights of the input layer and the hidden layer of the feed-forward NN, respectively and $W^{[3]}$ is the weight of the residual term.

For simplicity, one hidden layer is selected for the feed-forward NN and the hyperbolic tangent function is used for the activation function of a neuron. For any neuron of the hidden layer, we have $h_i(W_i^{[1]}\tilde{y}) = \tanh(W_i^{[1]}\tilde{y})$, where $i = 1,2,...,nn$ with nn being the neuron number; $W_i^{[1]}$ is the i-th row of $W^{[1]}$; and $h_i(W_i^{[1]}\tilde{y})$ is the i-th element of $h(W^{[1]}\tilde{y})$.

Then, an EID estimate $\hat{f}_e(t)$ is

$$\hat{f}_e(t) = \varphi_c(\tilde{y}) + u_f(t) - u(t). \tag{12}$$

As $\hat{f}_e(t)$ is a self-referential function, a filter $F(s)$ is employed to address this issue. Denote a state-space representation of $F(s)$ as

$$\begin{cases} \dot{x}_g(t) = A_g x_g(t) + B_g \hat{f}_e(t) \\ \tilde{f}_{e1}(t) = C_g x_g(t). \end{cases} \tag{13}$$

According to Fig. 1, the filtered estimate $\tilde{f}_e(t)$ is

$$\tilde{f}_e(t) = \tilde{f}_{e1}(t) + \alpha\varphi_c(\tilde{y}) \tag{14}$$

where α is a scalar to improve the stability.

V. LEARNING CONTROL OF DRNN-BASED ESTIMATOR

The learning control of the DRNN-based estimator is divided into two parts. The feed-forward NN is treated as a dynamic compensator. The residual term is treated as a performance-oriented adaptive learning control gain for the estimator, which is updated to reduce the impact of the nonlinearities and disturbances on the system output.

A. Dynamics of DRNN-Based Observer

Let the state error between the plant (1) and the observer (4) be

$$\tilde{x}(t) = x(t) - \hat{x}(t). \tag{15}$$

A combination of (1) and (4) gives

$$\begin{cases} \dot{\tilde{x}}(t) = A_L\tilde{x}(t) - B\tilde{f}_e(t) + B_f f(x(t),u(t),t) + B_d d_f(t) \\ \tilde{y}(t) = C\tilde{x}(t) \end{cases} \tag{16}$$

where

$$A_L = A - LC.$$

According to (13) and (14), we have

$$\begin{cases} \dot{x}_e(t) = A_e x_e(t) + B_e\varphi_c(\tilde{y}) \\ \tilde{f}_e(t) = C_e x_e(t) + D_e\varphi_c(\tilde{y}) \end{cases} \tag{17}$$

where $x_e(t) = x_g(t)$, $A_e = A_g + B_g C_g$, $B_e = B_g$, $C_e = C_g$, and $D_e = \alpha I$.

According to (11), combining (16) and (17) gives

$$\begin{cases} \dot{\psi}(t) = A_\psi\psi(t) + B_\psi\varphi_c(\tilde{y}) + B_{\psi f} f(x(t),u(t),t) + B_{\psi d} d_f(t) \\ \tilde{y}(t) = C_\psi\psi(t) \end{cases} \tag{18}$$

where

$$\begin{cases} \psi(t) = \begin{bmatrix} \tilde{x}(t) \\ x_e(t) \end{bmatrix}, A_\psi = \begin{bmatrix} A_L & -BC_e \\ 0 & A_e \end{bmatrix}, B_\psi = \begin{bmatrix} -BD_e \\ B_e \end{bmatrix} \\ B_{\psi f} = \begin{bmatrix} B_f \\ 0 \end{bmatrix}, B_{\psi d} = \begin{bmatrix} B_d \\ 0 \end{bmatrix}, C_\psi = \begin{bmatrix} C & 0 \end{bmatrix}. \end{cases} \tag{19}$$

Lemma 1: (*Kalman–Yakubovich–Popov* [1]) For a system $G(s) = (A,B,C,D)$ with (A,B) being controllable and (A,C) being observable, $G(s)$ is strictly positive real if and only if there exist matrices $P = P^T > 0$, W, M, and a positive constant ε such that the following equations hold:

$$\begin{cases} PA + A^T P = -M^T M - \varepsilon P \\ PB = C^T - M^T W \\ W^T W = D + D^T. \end{cases} \tag{20}$$

B. Learning Control of Feed-Forward NN

For performance-oriented estimation, the weights of the feed-forward NN are optimized by the backpropagation algorithm.

Theorem 1: The output of the feed-forward NN is bounded as long as the weight learning laws for the feed-forward NN are adopted by

$$\dot{W}^{[1]} = -\eta_1\kappa_1(\tilde{y}) - \rho_1 W^{[1]}, \tag{21}$$

$$\dot{W}^{[2]} = \begin{cases} -\eta_2\kappa_2(\tilde{y}) - \rho_2 W^{[2]}, & \text{for } \|W^{[2]}\| \le W_m^{[2]} \\ 0, & \text{for } \|W^{[2]}\| > W_m^{[2]} \end{cases} \tag{22}$$

where η_1, η_2 are the learning rates; ρ_1, ρ_2 are small positive numbers; $W_m^{[2]}$ is the bound of $W^{[2]}$; and

$$\begin{cases} \kappa_1(\tilde{y}) = \left(\tilde{y}^T \dfrac{\partial \tilde{y}}{\partial \varphi_c} W^{[2]} \Xi\right)^T \tilde{y}^T, \Xi = (I - h(W^{[1]}\tilde{y}) h^T(W^{[1]}\tilde{y})) \\ \kappa_2(\tilde{y}) = \left(\tilde{y}^T \dfrac{\partial \tilde{y}}{\partial \varphi_c}\right)^T h^T(W^{[1]}\tilde{y}), \dfrac{\partial \tilde{y}}{\partial \varphi_c} = C_\psi (e^{A_\psi t} - I) A_\psi^{-1} B_\psi. \end{cases} \tag{23}$$

Proof: Choose the cost function as

$$J = \frac{1}{2}\tilde{y}^T \tilde{y}. \tag{24}$$

On the other hand, $\frac{\partial J}{\partial W^{[2]}}$ and $\frac{\partial J}{\partial W^{[1]}}$ are

$$\begin{cases} \frac{\partial J}{\partial W^{[2]}} = \frac{\partial J}{\partial \tilde{y}} \frac{\partial \tilde{y}}{\partial \varphi_c} h^T(W^{[1]}\tilde{y}) = (\tilde{y}^T \frac{\partial \tilde{y}}{\partial \varphi_c})^T h^T(W^{[1]}\tilde{y}) \\ \frac{\partial J}{\partial W^{[1]}} = \frac{\partial J}{\partial \tilde{y}} \frac{\partial \tilde{y}}{\partial \varphi_c} \tilde{y}^T = (\tilde{y}^T \frac{\partial \tilde{y}}{\partial \varphi_c} W^{[2]} \Xi)^T \tilde{y}^T \end{cases} \tag{25}$$

where Ξ is given by (23).

According to (18), we have

$$\begin{aligned} \tilde{y} = {} & C_\psi e^{A_\psi t}\psi(0) - \int_0^t C_\psi e^{A_\psi (t-\tau)} B_\psi \varphi_c(\tilde{y}(\tau)) d\tau \\ & + \int_0^t C_\psi e^{A_\psi \tau} B_{\psi f} f(x(t-\tau), u(t-\tau), t-\tau) d\tau \\ & + \int_0^t C_\psi e^{A_\psi \tau} B_{\psi d} d_f(t-\tau) d\tau. \end{aligned} \tag{26}$$

Then, we have

$$\frac{\partial \tilde{y}}{\partial \varphi_c} = -\int_0^t C_\psi e^{A_\psi (t-\tau)} B_\psi d\tau = C_\psi (e^{A_\psi t} - I) A_\psi^{-1} B_\psi.$$

Consequently, we have the learning laws (21) and (22). Due to the boundedness of the weight $W^{[2]}$ by (21) and $\|h(W^{[1]}\tilde{y})\| \le 1$, the output $W^{[2]}h(W^{[1]}\tilde{y})$ of the feed-forward NN is bounded. This completes the proof.

□

C. Learning Control of Residual Term

A performance-oriented adaptive learning law is designed for the residual term with guaranteed stability in this subsection.

Theorem 2: The system of (18) is input-to-state stable as long as the system (A_ψ, B_ψ, C_ψ) is strictly positive real and the adaptive weight $W^{[3]}$ of the residual term is taken by

$$W^{[3]} = k\sigma^T(t) \tag{27}$$

where

$$\dot{\sigma} = -sign(k)\gamma \tilde{y}^T \tilde{y} - \beta\sigma \tag{28}$$

k is an nonzero number; and γ, β are positive numbers.

Proof: Choose a Lyapunov function as

$$V = \psi^T P \psi + \frac{|k|}{\gamma}\sigma^T\sigma \tag{29}$$

where $P = P^T > 0$. The derivative of V along the system of (18) is

$$\begin{aligned} \dot{V} = {} & \psi^T (PA_\psi + A_\psi^T P)\psi + 2\psi^T P B_\psi W^{[3]} + 2\frac{|k|}{\gamma}\sigma^T\dot{\sigma} \\ & + 2\psi^T P B_\psi \pi(\tilde{y}) + 2\psi^T P B_{\psi d} d_f + 2\psi^T P B_{\psi f} f \end{aligned} \tag{30}$$

where $\pi(\tilde{y}) = W^{[2]}h(W^{[1]}\tilde{y})$ is the output of the feed-forward NN. By Lemma 1, we have

$$\begin{aligned} \dot{V} = {} & -\psi^T(M^T M + \varepsilon P)\psi + 2\tilde{y}^T W^{[3]} + 2\frac{|k|}{\gamma}\sigma^T\dot{\sigma} \\ & + 2\psi^T P B_\psi \pi(\tilde{y}) + 2\psi^T P B_{\psi d} d_f + 2\psi^T P B_{\psi f} f. \end{aligned} \tag{31}$$

When the adaptive weight $W^{[3]}$ is selected as (27) we have

$$\begin{aligned} \dot{V} = {} & -\psi^T(M^T M + \varepsilon P)\psi - \frac{|k|}{\gamma}\beta\sigma^T\sigma + 2\psi^T P B_\psi \pi(\tilde{y}) \\ & + 2\psi^T P B_{\psi d} d_f + 2\psi^T P B_{\psi f} f. \end{aligned} \tag{32}$$

Using the following inequalities

$$2\psi^T P B_{\psi f} f \le \frac{\varepsilon}{4}\psi^T P \psi + \frac{4}{\varepsilon}(B_{\psi f} f)^T P B_{\psi f} f$$

$$2\psi^T P B_{\psi d} d_f \le \frac{\varepsilon}{4}\psi^T P \psi + \frac{4}{\varepsilon}(B_{\psi d} d_f)^T P B_{\psi d} d_f$$

$$2\psi^T P B_\psi \pi(\tilde{y}) \le \frac{\varepsilon}{4}\psi^T P \psi + \frac{4}{\varepsilon}(B_\psi \pi(\tilde{y}))^T P B_\psi \pi(\tilde{y}),$$

we have

$$\begin{aligned} \dot{V} \le {} & -\psi^T(M^T M + \frac{\varepsilon}{4}P)\psi + \frac{4}{\varepsilon}(B_{\psi f} f)^T P B_{\psi f} f - \frac{|k|}{\gamma}\beta\sigma^T\sigma \\ & + \frac{4}{\varepsilon}(B_{\psi d} d_f)^T P B_{\psi d} d_f + \frac{4}{\varepsilon}(B_\psi \pi(\tilde{y}))^T P B_\psi \pi(\tilde{y}). \end{aligned} \tag{33}$$

According to Theorem 1, the output of the feed-forward NN is bounded. For $f(x(t), u(t), t)$ and $d_f(t)$ satisfying Assumption 3 and Assumption 4, we have

$$\begin{aligned} \dot{V} \le {} & -(\lambda_{\min}(M^T M + \frac{\varepsilon}{4}P) - \frac{4}{\varepsilon}\lambda_{\max}(B_{\psi f}^T P B_{\psi f}) R^2)\|\psi\|^2 \\ & - \frac{|k|}{\gamma}\beta\sigma^T\sigma + \frac{4}{\varepsilon}\lambda_{\max}(B_{\psi d}^T P B_{\psi d}) d_m^2 + \frac{4}{\varepsilon}\lambda_{\max}(B_\psi^T P B_\psi)(W_m^{[2]})^2. \end{aligned}$$

Therefore, the system of (18) is input-to-state stable [1]. This completes the proof. □

VI. Stability analysis of closed-loop system

This section summarizes a robust stability condition by Theorems 1 and 2.

Theorem 3: When the matrix A_ψ of (19) and the matrix A_K of (9) are designed to be stable; the system (A_ψ, B_ψ, C_ψ) is strictly positive real; and the weights are selected by (21), (22), and (27), then the DRNN-based closed-loop system is uniformly ultimately bounded stable.

The proof is clear. So it is omitted here.

A closed look clarifies that the system (A_ψ, B_ψ, C_ψ) is actually the series system of the system $(A_L, -B, C)$ and the system (A_e, B_e, C_e, D_e). To make the series system (A_ψ, B_ψ, C_ψ) stable, A_e should be selected to be stable. Summarizing the key findings leads to the design procedure outline as illustrated in the Algorithm 1 for the developed DRNN-based control system.

VII. Simulations and analysis

In this section, we apply the developed method to a single-joint robot system. The single-joint robot contains one joint and one rigid link, and its physical structure is shown in Fig.

Algorithm 1: Learning Control Design Algorithm

Design K_p and L such that A_K of (9) and A_L of (16) are stable, respectively;
Select the filter (A_g, B_g, C_g) such that A_e is stable;
repeat
  Select α;
until *The system (A_ψ, B_ψ, C_ψ) of (18) is strictly positive real*;
repeat
  Select k,γ, and β for the adaptive learning law (27) and (28);
  Select $\eta_1, \eta_2, \rho_1, \rho_2$;
  Initiate $W^{[1]}(0), W^{[2]}(0)$ within $[-1, 1]$;
  Train the DRNN;
until *The disturbance-rejection performance is satisfactory*;
End.

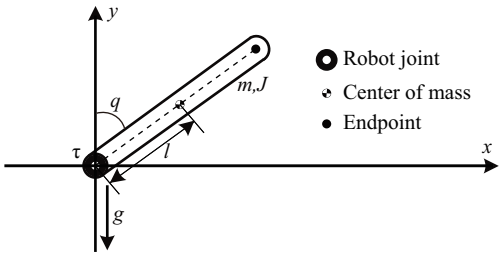

Fig. 3. Physical structure of the single-joint robot.

3, where q is the angle of the link relative to the vertical axis; m is the mass of the link; l is the distance from the robot joint to the center of mass of the link; J is the moment of inertia relative to the link shaft; and τ is the torque of the motor.

The Euler–Lagrange model [16] of the single-joint robot is

$$(ml^2 + J)\ddot{q} + mgl\sin(q) = \tau + d \tag{34}$$

where d denotes joint friction and exogenous disturbance.

The value of the system parameters in (34) are

$$\begin{cases} m = 0.7980 \text{ kg},\ l = 0.1238 \text{ m} \\ g = 9.80 \text{ m/s}^2,\ \text{J} = 0.0198 \text{ kg}\cdot\text{m}^2. \end{cases} \tag{35}$$

Let $x_1 = q, x_2 = \dot{q}$, $u = \tau$, and $y = x_1 + x_2$. The parameters in the state-space model (1) are

$$\begin{cases} A = \begin{bmatrix} 0 & 1 \\ 0 & 0 \end{bmatrix},\ B = B_f = \begin{bmatrix} 0 \\ 31.234 \end{bmatrix},\ B_d = \begin{bmatrix} 1 \\ 1 \end{bmatrix} \\ C = \begin{bmatrix} 1 & 1 \end{bmatrix},\ f(x(t), u(t), t) = 0.9682\sin(x_1(t)). \end{cases} \tag{36}$$

Let the disturbance be

$$d_f(t) = 10, \quad 3 \le t \le 7. \tag{37}$$

Use the linear quadratic regulation (LQR) method to design K_p and L such that A_K and A_L are Hurwitz. The corresponding weighting matrices are

$$\begin{cases} Q_K = \text{diag}\{10, 10\}, \quad R_K = 1 \\ Q_L = \text{diag}\{1000, 1000\}, \quad R_L = 1 \end{cases}$$

which give

$$K_p = [-3.1623 \quad -3.1941],\ L = [13.800 \quad 31.623]. \tag{38}$$

As the conventional EID estimator, the low-pass filter $F(s)$ is selected as

$$F(s) = \frac{100}{s + 100.1}. \tag{39}$$

To ensure the system (A_ψ, B_ψ, C_ψ) of (18) is strictly positive real, α is selected as

$$\alpha = -1000.$$

For the DRNN-based estimator, by trial and error, the parameters are chosen as

$$\begin{cases} k = 10,\ \gamma = 10^6,\ \beta = 1 \\ \eta_1 = 0.0010, \eta_2 = 0.0010, \rho_1 = 0.0002, \rho_2 = 0.0002. \end{cases}$$

Choose 5 neurons for the hidden layer of the feed-forward NN and let the initial values $W^{[1]}(0)$, $W^{[2]}(0)$ be random numbers within the range $[-1, 1]$. Train the feed-forward NN five times for proper initial weights and the final weights are

$$\begin{cases} W^{[1]}(t_f) = [0.3318, -0.0910, -0.1065, -0.9678, 0.7232] \\ W^{[2]}(t_f) = [0.8751, -0.0423, 0.1399, 0.9871, -0.1932]. \end{cases}$$

where $t_f = 10$ s is the final time.

To validate the developed method in the real environment, bandwidth-limited white noise with a signal-noise ratio being about 40 dB and a sampling time being 0.01 s is added to the system output. The output response is shown in Fig. 4. The output almost has no error during the whole process. It is worth noting the developed DRNN-based learning estimator has remarkable dynamic performance when the large force is imposed at the 3th s and then removed at the 7th s.

The disturbance-rejection performance of the DRNN-based system is compared with the conventional EID-based system [15]. To be fair, the state-feedback control gain, the observer gain, and the bandwidth of the first-order filter are the same as the DRNN-based control system. For comparison, the results of the proceeding two methods are shown in Fig. 5.

Although the conventional EID method is able to provide a similar steady-state performance, the overshoots of the control action and system output are near zeros, which are far less than those of the conventional EID method. This is an incomparable advantage.

VIII. Conclusion

To enhance the learning or estimation performance for unknown nonlinearities and disturbances, this paper appropriately integrated a DRNN into an EID-based control system. First, an auxiliary indicator was used to evaluate the impact of nonlinearities and disturbances on the system output. Then, a DRNN was integrated into a conventional EID

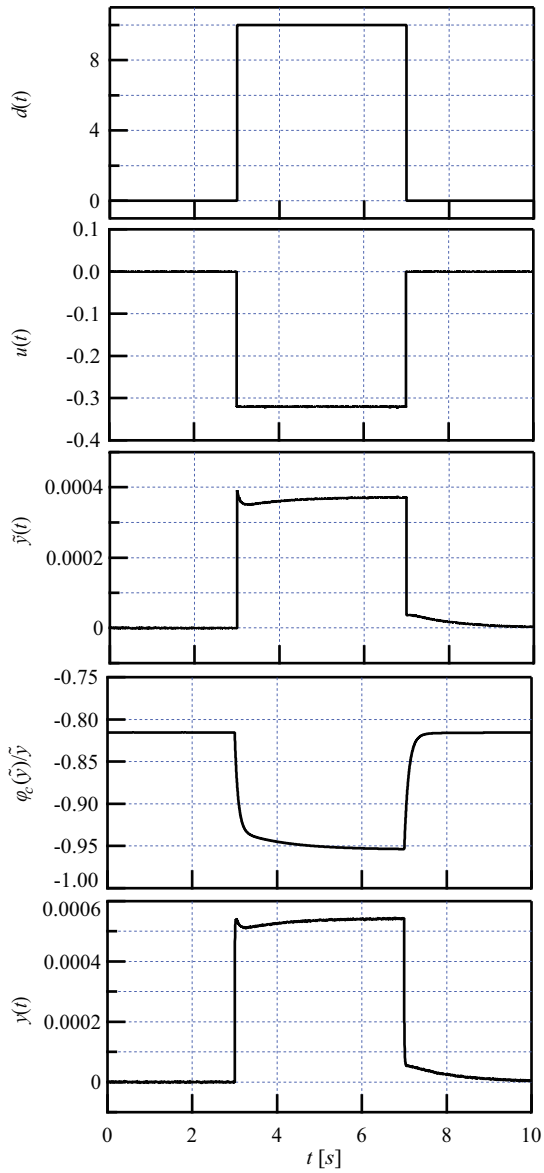

Fig. 4. System response of DRNN-based control system.

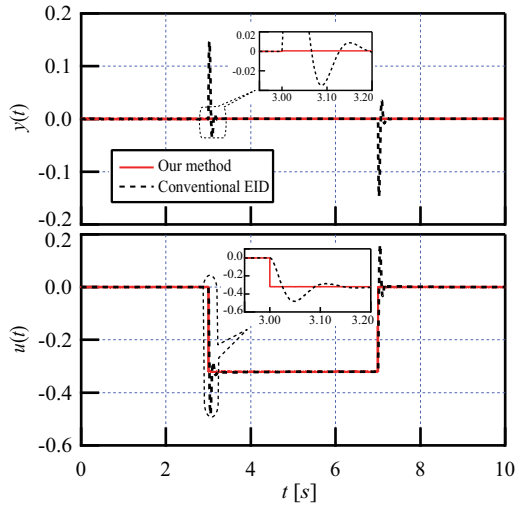

Fig. 5. Comparison results for DRNN-based and EID-based control systems.

estimator framework. This methodology utilized a residual term as a performance-focused adaptive learning mechanism to ensure stability. The feed-forward NN acted as a dynamic learning compensator, refined through backpropagation optimization. Finally, the efficacy and superior performance of the DRNN-based estimator were demonstrated on a single-joint robot system.

REFERENCES

[1] H. K. Khalil, *Nonlinear Systems*. Upper Saddle River, NJ, USA: PrenticeHall, 2002.

[2] X. Lu and H. Li, "A hybrid control approach to H_∞ problem of nonlinear descriptor systems with actuator saturation," *IEEE Trans. Autom. Control.*, vol. 66, no. 10, pp. 4960-4966, Oct. 2021.

[3] S. Roy, S. Baldi, and L. M. Fridman, "On adaptive sliding mode control without a priori bounded uncertainty," *Automatica*, vol. 111, Jan. 2020, Art. no. 108650.

[4] S. Byeon and G. Park, "Safe and robust stabilization of uncertain nonlinear systems via control lyapunov-barrier function and disturbance observer: a preliminary study," *Proc. 62nd IEEE Conf. Decis. Control (CDC)*, pp. 6525–6532, 2023.

[5] J. Y. Lau, W. Liang, and K. K. Tan, "Motion control for piezoelectric-actuator-based surgical device using neural network and extended state observer," *IEEE Trans. Ind. Electron.*, vol. 67, no. 1, pp. 402-412, Jan. 2020.

[6] P. Yu, Q. Wu, K. -Z. Liu, J. She, and X. Li, "Tunable nonlinear-function-based estimators for mismatched disturbances and performance analysis," *IEEE Trans. Ind. Electron.*, vol. 71, no. 9, pp. 11453-11464, Sept. 2024.

[7] E. Sariyildiz, R. Oboe, and K. Ohnishi, "Disturbance observer-based robust control and its applications: 35th-anniversary overview," *IEEE Trans. Ind. Electron.*, vol. 67, no. 3, pp. 2042–2053, Mar. 2020.

[8] L. Nie, M. Zhou, W. Cao, and X. Huang, "Improved nonlinear extended observer based adaptive fuzzy output feedback control for a class of uncertain nonlinear systems with unknown input hysteresis," *IEEE Trans. Fuzzy Syst.*, vol. 31, no. 10, pp. 3679-3689, Oct. 2023.

[9] A. Liu and T. Li, "Distributed platoon control of nonlinear vehicles with event-triggered extended state observers: closed-loop stability," *Proc. 61nd IEEE Conf. Decis. Control (CDC)*, pp. 1734-1739, 2022.

[10] J. She, M. X. Fang, Y. Ohyama, H. Kobayashi, and M. Wu, "Improving disturbance-rejection performance based on an equivalent-input-disturbance approach," *IEEE Trans. Ind. Electron.*, vol. 55, no. 1, pp. 380–389, Jan. 2008.

[11] X. Yin, J. She, M. Wu, D. Sato, and K. Ohnishi, "Disturbance rejection using SMC-based-equivalent-input-disturbance approach," *Appl. Math. Comput.*, vol. 418, Apr. 2022, Art. no. 126839.

[12] P. Yu, Q. Wu, K. -Z Liu, and J. She, "Multi-objective design of parametric equivalent-input-disturbance approaches with application to vehicle suspension systems," *J. Franklin Inst.*, vol. 361, no. 10, Jul. 2024.

[13] A. H. Khan, S. Li, and X. Luo, "Obstacle avoidance and tracking control of redundant robotic manipulator: an RNN-based metaheuristic approach," *IEEE Trans. Ind. Inform.*, vol. 16, no. 7, pp. 4670-4680, July 2020.

[14] A. H. Khan, S. Li, D. Chen, and L. Liao, "Tracking control of redundant mobile manipulator: an RNN based metaheuristic approach," *Neurocomputing*, vol. 400, pp. 272–284, Aug. 2020.

[15] P. Yu, K. Liu, J. H. She, and M. Wu, "Robust disturbance rejection for repetitive control systems with time-varying nonlinearities," *Int. J. Robust Nonlinear Control.*, vol. 29, no. 5, pp. 1597–1612, Jan. 2019.

[16] Lynch, Kevin M., and Frank C. Park. *Modern robotics*. Cambridge University Press, 2017.